Available online at www.sciencedirect.com

SciVerse ScienceDirect

Procedia Engineering 59 (2013) 51 – 58

Procedia Engineering

www.elsevier.com/locate/procedia

3rd International Conference on Tissue Engineering, ICTE2013

Bio-Inspired ceramics: promising scaffolds for bone tissue engineering

M. López-Álvarez*, C. Rodríguez-Valencia, J. Serra, P. González

Grupo Nuevos Materiales, Instituto de Investigación Biomédica de Vigo, Escuela de Ingenieros Industriales, Campus Lagoas-Marcosende, Universidade de Vigo, Vigo 36310, Spain

Abstract

Three-dimensional scaffolds for bone tissue engineering should replicate bone architecture with hierarchical and interconnected pores distribution to promote neobone tissue ingrowth, blood vessel invasion and nutrient delivery. Ceramic scaffolds of silicon carbide (SiC) and pyrolyzed carbon (C), both obtained from plant precursors, present an abundant macro, meso and nanoscaled porosity, maintained from the natural structures. Obtaining of SiC and C scaffolds from wood of *Entandrophragma cylindricum*, macroalgae *Laminaria ochroleuca* and marsh plant *Juncus maritimus* and physicochemical characterization were carried out. Cells morphology, proliferation and osteogenic activity were successfully evaluated in all ceramic scaffolds with MC3T3-E1 pre-osteoblasts up to 28 days.

Selection and peer-review under responsibility of the Centre for Rapid and Sustainable Product Development, Polytechnic Institute of Leiria, Centro Empresarial da Marinha Grande.

Keywords: Bio-inspired porous ceramics; Silicon carbide; Carbon scaffolds; MC3T3-E1; Osteogenic activity.

* Corresponding author. Tel.: +34 986 812 216; fax: +34 986 812 201.
E-mail address: miriammsd@uvigo.es

Selection and peer-review under responsibility of the Centre for Rapid and Sustainable Product Development, Polytechnic Institute of Leiria, Centro Empresarial da Marinha Grande
doi:10.1016/j.proeng.2013.05.093

1. Introduction

The designing of three-dimensional scaffolds to provide solutions for the replacement, repair and regeneration of specific human organs and tissues represents, currently, one of the main pillars in the tissue engineering research. In the case of bone, scaffolds should replicate its architecture and three dimensional structures with predetermined density, hierarchical pore distribution and interconnected pathways. Thus, in relation with pores, they will promote migration and proliferation of osteoblasts and mesenchymal cells, neobone tissue ingrowth, efficient *in vivo* blood vessel invasion, nutrient delivery and matrix deposition in empty spaces. As it has been previously demonstrated macropores (size >100 μm) have a critical impact on osteogenic outcomes, promotion of vascularization and mass transportation of nutrients and waste products [1], micropores will favor capillary formation and, finally,

nanopores will allow diffusion of molecules for nutrition and signaling [2] and favor the adsorption of proteins for the cells anchorage [3].

Different ceramics have been proposed for these applications but especially the family of calcium phosphates (tricalcium phosphate, TCP, hydroxyapatite, substituted apatite, biphasic systems) which, in addition to the bioactive properties, have a similar composition to the mineral part of bone and are bioresorbable. This has represented an important advantage for filling bone defects [4] although implies a correlation between the rate of resorption of the ceramic and the rate of bone regeneration, and it does not always occur [5]. Calcium phosphates are characterized by being capable of forming a strong bone-implant interface and biologically close, avoiding the formation of fibrous tissue that encapsulates the implant isolating it from the organism and often causing it loss, thus, the most common application is as a coating for orthopaedic metal implants in places requiring a strong interface. It is, however, a material incapable of sustaining a significant load.

Non-oxide ceramics as silicon carbide has experienced a growing interest last years. These ceramics present practically no sensitivity to fracture, are very stable chemically, resist high temperatures and have a much higher hardness. In addition, the porous ceramics of silicon carbide will promote the new bone ingrowth into the scaffold and the subsequent improvement of osteointegration in the body [3]. These porous SiC has been obtained from wood precursors to orthopedic applications and its chemically inert behavior, also with the interconnected and hierarchical porosity preserved from the plant vascular system were successfully evaluated [6-8].

Thus, biodiversity represents an enormous potential for obtaining suitable three-dimensional porous bio-structures. Moreover, the biodiversity of the natural grown plant structures offers a large variety of templates with different density, morphology, pore shape, pore size, and interconnection, surface patterning that meet the requirements to obtain bio-inspired materials for scaffold applications. Currently, several authors have proposed the use of different marine species like coral skeletons, sea urchins and sponges as three dimensional biomatrices [9-13]. The results confirmed that the three dimensional topography, the porosity and the surface parameters of these materials influence positively in the cell differentiation.

On the other hand, ceramic scaffolds of pyrolytic carbon present also great perspectives at the biomaterials field. In fact, the use of carbon in the biomedical field, in the form of nanotubes and nanofibers, has experienced an increasing interest in the last 10 years due to its composition, morphology and physical–electrical properties [3,14,15]. In addition to these more recent applications, the use of carbon in the biomedical industry dates back to the late sixties when the unique blood compatibility of pyrolytic carbon as well as its physical and mechanical properties allowed, since 1968, its use in heart valve components (DeBakey-Surgitool®) and as a coating on vascular grafts [2,16,17].

In the present work, obtaining and physicochemical characterization of SiC and C scaffolds from wood of *Entandrophragma cilindricum*, the macroalgae *Laminaria ochroleuca* and the marsh plant *Juncus maritimus* were carried out. At the same time *in vitro* biocompatibility was evaluated by the pre-osteoblastic cell line MC3T3-E1 up to 28 days to analyze cells morphology, proliferation and osteogenic activity.

2. Materials and Methods

The fabrication of silicon carbide and carbon scaffolds obtained from these plant precursors *Entandrophragma cylindricum, Laminaria ochroleuca* and *Juncus maritimus* consisted on their pyrolysis or thermal decomposition to obtain the carbon scaffold and the further reactive infiltration of them with molten silicon at 1550ºC to obtain the silicon carbide scaffolds. Parameters and atmosphere conditions have been optimized depending on the precursor of origin and described before [18-20].

The secondary-electron imaging of the microstructure of the C and SiC scaffolds obtained was performed using a scanning electron microscope (SEM) (Philips XL30; CACTI, University of Vigo). This technique was also used in the biocompatibility studies to analyze the morphology of the cells during their spreading and proliferation, for each time of culture. The structural characterization was carried out with X-ray diffraction (XRD) and Infrared Fourier transformed spectroscopy (FT-IR). The XRD technique was used to identify the crystalline components and phases. The equipment used was a Siemens D-5000 Diffractometer (CACTI, University of Vigo). Functional groups in the IR range were identified using a FTIR Bomem MB-100 spectrometer (CACTI, University of Vigo).

Samples were sterilized with the application of several 15 min ultrasound baths, starting with milli-Q water, followed by 70% ethanol and acetone and autoclaved at 121ºC for 20 min. Solvents from the materials were firstly extracted to evaluate their potential release of cytotoxic particles by rolling the samples immersed in MEM-alpha (Sigma, USA) with 10% of Fetal Bovine serum (FBS; Invitrogen, USA) and 1% of Antibiotic/Antimicotic solution during 90 hours at 37ºC and in rolling. A surface area of material to volume ratio of 2 cm^2/ mL was used. The extracted solvents were then diluted with fresh cellular growth medium to obtain dilutions of 0, 20, 30, 50 and 100% of the extract. The same procedure was followed with phenol solution at 6.4g/l and with supplemented growth medium as positive and negative controls, respectively. Finally different dilutions, including controls, were incubated for 24 hours with monolayers of the pre-osteoblastic cell line MC3T3-E1 (ECACC, U.K.) and cellular viability was evaluated by means of the Cell Proliferation Kit I from Roche Molecular Biochemicals (MTT assay).

For direct contact assays a cell suspension of MC3T3-E1 of 1.7×10^5 cells ml−1 in 100 µl of MEM-alpha supplemented with 10% fetal bovine serum was added directly on the surface of the sterilized samples. Previously, the scaffolds were placed in 96-well tissue culture plates. Cells were cultured up to 28 days in a humidified atmosphere with 5% CO_2 and at 37°C. To induce the differentiation 1 day after seeding, ascorbic acid 2-phosphate (2 mM) and glycerol 2-phosphate (10 mM) were added to the MEM-alpha, and 7 days after the cell seeding melatonin solution (50 nM) was also added. The culture medium was renewed every 2–3 days.

Cell morphology was analyzed by SEM Philips XL30 as described elsewhere [20]. The cellular cytoskeleton was observed by confocal laser scanning microscopy (CLSM) Bio-Rad MRC 1024 where cells were fixed with a solution of paraformaldehyde as described elsewhere [20] and Alexa fluor 488 phalloidin and propidium iodide solutions were added to visualize the cellular cytoskeletal actin filaments and cell nuclei, respectively. Cells proliferation was evaluated by the MTT Assay as described elsewhere [20].

3. Results and Discussion

As an example of the natural structures and the C and SiC obtained ceramics, it is shown this selection of different precursors (Figure 1), but it is important to note that all plant-derived structures tested behave similarly. Thus, Figure 1 shows SEM micrographs of the cross section of natural plant *Juncus maritimus* (a,b), the porous carbon of *Laminaria ochroleuca* (c,d) and the bio-inspired silicon carbide of *Entandrophragma cilindricum* (e,f) at two different magnifications for each material. In the micrographs of the natural plant (Fig 1a,b) it can be observed as cross section presents vascular bundles with pores of 20-25 µm that correspond to xylem (Fig 1a) and of <5µm which are phloem (Fig 1b). Both of them are distributed through the whole section of the plant communicating the central section with the most external layer of the epidermis.

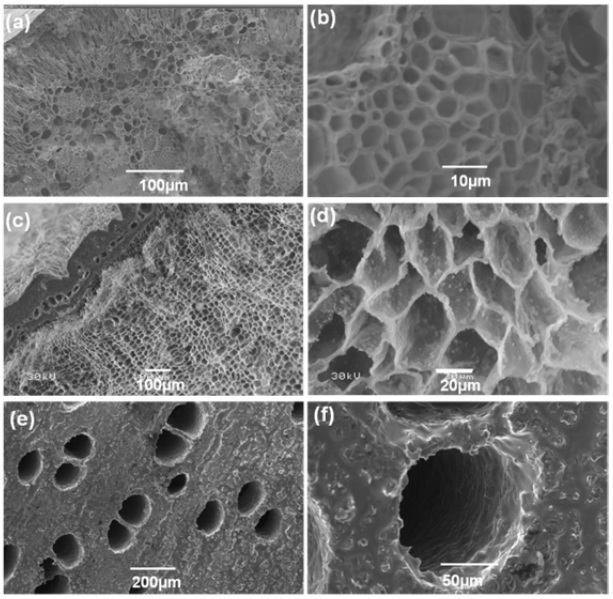

Fig.1. SEM micrographs at two different magnifications of *Juncus maritimus* (a,b), porous carbon of *Laminaria ochroleuca* (c,d) and bio-inspired silicon carbide of *Entandrophragma cylindricum* (e,f).

The bio-inspired carbon obtained from the stipe of *Laminaria ochroleuca* (Fig 1c,d) presents also a uniform distribution of pores through the entire cross section, with pores of 40-50 µm distributed along the periphery and pores slightly smaller and very abundant with a homogeneous distribution in the remaining (Fig 1c) presented in a higher magnification and detail in Fig 1d. Finally, the morphological characterization of silicon carbide obtained from *Entandrophragma cilindricum* (Fig 1e,f) evidenced the particular porous microstructure of this tree. Macropores of around 80 µm disposed in groups of two or three, characteristic of this tree, can be seen at the surface of the cross section of the SiC (Fig 1e). One of these pores is presented in detail in Fig 1f.

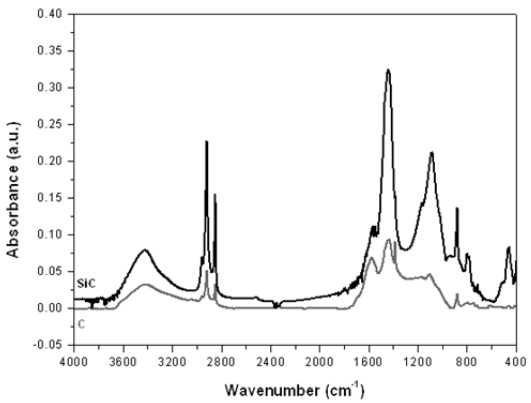

Figure 2 FT-IR spectra of carbon and silicon carbide obtained from *Juncus maritimus*.

Carbon and silicon carbide scaffolds obtained from the different precursors were characterized by FT-IR. As an example in Figure 2 it is presented the spectra obtained for *J. maritimus*. The main IR absorption bands can be attributed to the following functional groups [21-23]: C-H groups exhibit sharp peaks located between 2800 and

2960 cm^{-1} associated to C-H_2 symmetric stretching (2860-2875 cm^{-1}), C-H_2 asymmetric stretching (2910-2930 cm^{-1}) and C-H_3 symmetric stretching (2950-2960 cm^{-1}). Moreover, well resolved peaks attributed to CH_3 symmetric and asymmetric bending modes emerge at around 1380 and 1436 cm^{-1}, respectively. Carbonate groups can be identified by two absorption bands; the peak of around 877 cm^{-1} associated to C-O bending vibration out-of-plane and 750 cm^{-1} related to C-O bending vibration in-plane. Other band at 1568 cm^{-1} can be associated to C=O stretching mode corresponding to carboxyle groups.

The broad absorption band of absorbed water can be observed in the range 3200-3700 cm^{-1} (water stretching vibration). The hydroxyl group (-OH) has a stretching vibration mode that appears at around 3571 cm^{-1} with a shoulder at 3550 cm^{-1}. In the case of the IR analysis of SiC scaffolds and besides of the previous described bands, new absorption peaks can be identified; SiC groups around 782 and 798 cm^{-1} associated to Si-C stretching vibration mode and Si-O groups which exhibit bands located around 1100 cm^{-1}, 800 cm^{-1} and 450 cm^{-1} identified as symmetric stretching, bending and rocking vibration modes respectively.

The composition of the silicon carbide ceramics was evaluated in terms of crystallinity by XRD as indicates the Figure 3 where the spectra of the SiC ceramics obtained from *Entandrophragma cilindricum* (a), *Laminaria ochroleuca* (b) and *Juncus maritimus* (c) are presented. As it can be observed the three spectra confirmed the composition of the ceramics by the presence of the diffraction peaks corresponding to SiC, more particularly, the β-SiC cubic polytype [24]. At the same time residual silicon was detected that is accumulated in the surrounding of the SiC crystals. In the SiC spectrum of *J. maritimus* it was also detected the presence of silicon dioxide, formed due to the low vacuum conditions established in its case, and aluminum that can be introduced from the melting pot (made of this material) used to introduce the sample into the furnace for the reactive infiltration at 1550ºC of molten silicon with the carbon structure.

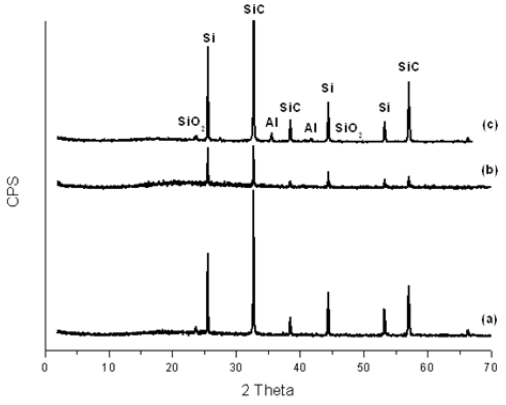

Figure 3 XRD spectra of silicon carbide ceramics obtained from *Entandrophragma cilindricum* (a), *Laminaria ochroleuca* (b) and *Juncus maritimus* (c).

The biological behavior of these bioinspired materials was assessed using several in vitro assays. Figure 4 presents the solvent extraction test results for the porous carbon scaffold obtained from *L. ochroleuca* in a plot of the optical density, which is proportional to the cell viability, against the different dilutions of the extracts obtained from the material and controls. It was observed that, when a dilution of 20% of each extract in fresh medium was added to the cells, the optical density in the positive control (cytotoxic) presented values close to zero what validated the experiment. In case of the carbon extracts the cell viability was maintained constant up to the 100% of extract added, in case of the negative control of cytotoxicity (cell growth media) the cells viability presented the same values as the carbon of *L. ochroleuca* being higher when the 100% was added. These results clearly demonstrated the non cytotoxicity of the extracts obtained from the porous carbon of *L. ochroleuca*, where no detrimental effects on the MC3T3-E1 pre-osteoblasts viability was observed at any dilution tested. Similar results were achieved for the rest of materials obtained from the other precursors.

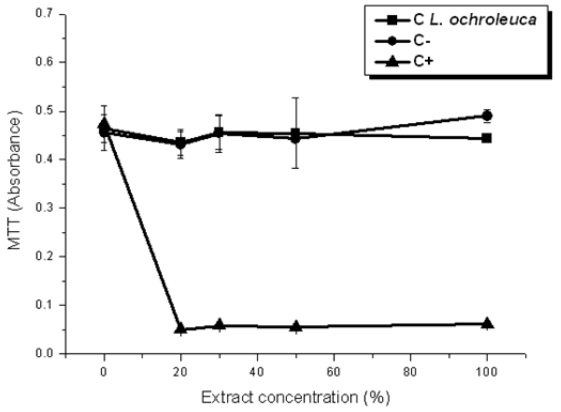

Figure 4 Solvent extraction test of the bio-inspired carbon obtained from *L. ochroleuca*

The pre-osteoblastic cell line MC3T3-E1 morphology, evaluated by scanning electron microscopy (SEM) on the SiC obtained from *Entandrophragma cilindricum*, is presented in Figure 5 after 1 day of incubation (a), 7 days (b) and 28 days (c,d). Thus, after one day of incubation cells appeared closely attached to the SiC ceramics with the flattened morphology typical of healthy osteoblasts starting to colonize the pores. When observed on the 7th day of incubation (Fig 5b) several layers of cells covered the surface, cells attached and spread properly, without any signal of cytotoxicity. Finally, after 28 days of cell culture (Fig 5c,d) micrographs showed as pre-mineralized extracellular matrix with a complex network of filopodia (Fig 5c) and constituents of the ECM (Fig 5d) were observed.

Finally the morphology of the patterned surfaces of the carbon scaffolds obtained from the marine plant *J. maritimus* and the MC3T3-E1 cells morphology when cultured on them for 24 hours were assessed by SEM and CLSM analysis, respectively, and presented in Figure 6. Thus, as it can be observed in Fig 6a and b, the surface presents a double patterning with macro-ridges of 100 μm in width containing micro-ridges of about 7 μm in width. Both oriented in the longitudinal direction and maintained from the plant of origin. Figure 6c and d presents the cytoskeleton of the cells after 24 h of incubation analyzed by CLSM. The cell nuclei are seen in red and the actin filaments of the cytoskeleton in green. The alignment of the cells, marked by the orientation of actin filaments following the direction determined by the channels, can be observed. Some of the nuclei acquire an oval shape as a result of the expansion of the cell.

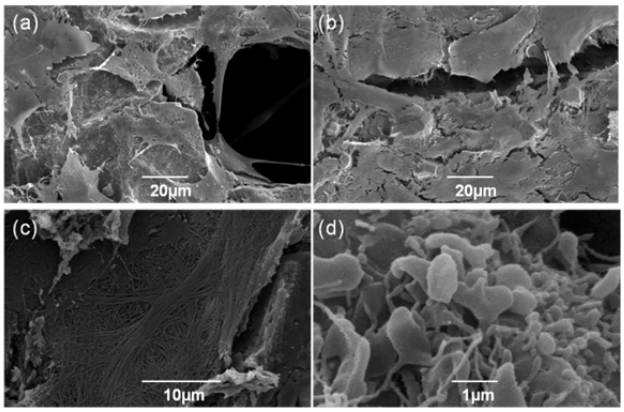

Figure 5 SEM micrographs of MC3T3-E1 pre-osteoblasts after 1 day of incubation (a), 7 days (b) and 28 days (c,d) on SiC obtained from Entandrophragma cilindricum.

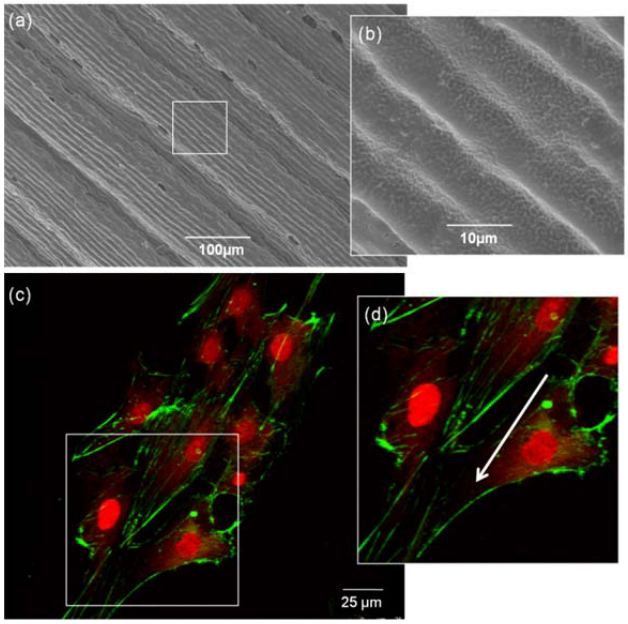

Figure 6. SEM micrographs in two magnifications of the patterned surface of C scaffold from J. maritimus (a,b) and CLSM images of cells cytoskeleton after 24 h of incubation on the patterned surface of C scaffold where the cell nuclei and F-actin filaments were stained in red and green, respectively (c,d) (Taken from [19]).

4. Conclusion

This paper aimed to demonstrate the enormous potential provided by the different plant precursors, such as wood (in this case *Entandrophragma cilindricum*), plants (*J. maritimus*) and macroalgae (*Laminaria ochroleuca*), for their application as biocompatible scaffolds for tissue engineering, oriented in the present work to the bone tissue regeneration being successfully tested with MC3T3-E1 pre-osteoblasts. Thus, these natural precursors were able to be processed to ceramic materials (pyrolytic carbon or silicon carbide) while retaining the porosity of vascular system of the plant source and the surface patterning or any other structural features already elaborated in Nature and generally very hard and expensive to be reproduced artificially.

Acknowledgements

Authors want to acknowledge UE-INTERREG 2011-1/164MARMED and Ministerio de Ciencia (MAT2010-18281) projects. M. López-Álvarez thanks funding support from FP7/REGPOT-2012-2013.1 nº 316265, BIOCAPS project.

References

[1] Wang, J.H.C., Grood, E.S., Florer, J., Wenstrup, R., 2000. Alignment and proliferation of MC3T3-E1 osteoblasts in microgrooved silicone substrata subjected to cyclic stretching, Journal of Biomechanics 33, p. 729.
[2] Ratner, B.D., 2004. A history of biomaterials, in "Biomaterials Science: An Introduction to Materials in Medicine" B.D. Ratner, A.S. Hoffmann, F.J. Schoen, Editors. Elsevier, London, p. 10.
[3] Karageorgiou, V., Kaplan, D., 2005. Porosity of 3D biomaterial scaffolds and osteogenesis, Biomaterials 26, p. 5474.
[4] Chevalier, J., Gremillard, L., 2009. Ceramics for medical applications: A picture for the next years, Journal of the European Ceramic Society 29, p. 1245.
[5] Ginebra, M.P., Espanol, M., Montufar, E.B., Pérez, R.A., Mestres, G., 2010. New processing approaches in calcium phosphate cements and their applications in regenerative medicine, Acta Biomaterialia 6(8), p. 2863.

[6] Borrajo, J.P., Serra, J., Liste, S., González, P., Chiussi, S., León, B., Pérez-Amor, M., 2005. Pulsed laser deposition of hydroxylapatite thin films on biomorphic silicon carbide ceramics, Applied Surface Science 248(1-4), p. 355.
[7] Varela-Feria, F.M., López-Robledo, M.J., Martínez-Fernández, J., de Arellano-López A.R., Singh, M., 2002. Precursor selection for property optimization in biomorphic SiC ceramics, Ceramic Engineering and Science Proceedings 23, p. 681.
[8] González, P., Serra, J., Liste, S., Chiussi, S., León, B., Pérez-Amor, M., Martínez-Fernández, J., de Arellano-López, A.R., Varela-Feria, F.M., 2003. New biomorphic SiC ceramics coated with bioactive glass for biomedical applications, Biomaterials 24(26), p. 4827.
[9] Abramovitch-Gottlib, L., Geresh, S., Vago, R., 2006. Biofabricated marine hydrozoans: A bioactive crystalline material promoting ossification of mesenchymal stem cells, Tissue Engineering 12(4), p. 729.
[10] Green, D.W., 2008. Tissue bionics: examples in biomimetic tissue engineering, Biomedical Materials 3, p. 1.
[11] Cunningham, E., Dunne, N., Walker, G., Maggs, C., Wilcox, R., Buchanan, F., 2010. Hydroxyapatite bone substitutes developed via replication of natural marine sponges, Journal of Materials Science: Materials in Medicine 21(8), p. 2255.
[12] Huebsch, N., Mooney, D.J., 2009. Inspiration and application in the evolution of biomaterials, Nature 462, p. 426.
[13] Lakes, R., 1993. Materials with structural hierarchy, Nature 361, p. 511.
[14] Gómez de Salazar, J.M., Barrena, M.I., Merino, C., Plaete, O., Morales, G., 2007. Preparación y estudio de materiales compuestos nanofibras de carbono/poliéster laminados con fibra de vidrio, Anales de la Mecánica de Fractura 1, p. 234.
[15] Harrison, B.S., Atala, A., 2007. Carbon nanotube applications for tissue engineering, Biomaterials 28, p. 344.
[16] More, R.B., Haubold, A.D., Bokros, J.C., 2004. Pyrolytic carbon for long-term medical implants, in "Biomaterials science: an introduction to materials in medicine" B.D. Ratner, A.S. Hoffmann, F.J .Schoen, Editors. Elsevier, London, p. 170.
[17] McChaney, J.M., Banas, C.E., 1996. Carbon containing vascular graft and method for making same. US Patent 009157.
[18] López-Álvarez, M., Pereiro, I., de Carlos, A., Serra, J., Gonzalez, P., 2012. Porous silicon carbide scaffolds with patterned surfaces obtained from the sea rush Juncus maritimus for tissue engineering applications, International Journal of Applied Ceramics Technology 9(3), p. 486.
[19] López-Álvarez, M., Pereiro, I., Serra, J., de Carlos, A., González, P., 2011.Osteoblast-like cell response to macro and micro-patterned carbon scaffolds obtained from the sea rush Juncus maritimus, Biomedical Materials 6(4), p. 045012.
[20] López-Álvarez, M., de Carlos, A., González, P., Serra, J., León, B., 2010. Cytocompatibility of bio-inspired silicon carbide ceramics, Journal of Biomedical Materials Research Part B: Applied Biomaterials 95(1), p. 177.
[21] Smith, B., 1999. Infrared Spectral Interpretation A Systematic Approach, CRC Press, Boca Raton Florida.
[22] Dragnea, B., Boulmer, J., Débarre, D., Bourguignon, B., 2001. Growth of a SiC layer on Si(100) from adsorbed propene by laser melting, Journal of Applied Physics 90, p. 449.
[23] Qian, J.M., Jin, Z.H., 2006. Preparation and characterization of porous, biomorphic SiC ceramic with hybrid pore structure, Journal of the European Ceramic Society 26, p. 1311.
[24] Dressler, W., Riedel, R., 1997. Progress in silicon-based non-oxide structural ceramics, International Journal of Refractory Metals and Hard Materials 15, p. 13.